Open access • Posted Content • DOI:10.1101/2020.05.22.111716

3D-Construction of Vasculature of Anaxagorea and its Implications in the Integrated Axial-Foliar Origin of the Angiosperm Carpel — Source link

Ya Li, Wei Du, Shuai Wang, Xiao-Fan Wang ...+1 more authors

Institutions: Wuhan University, Hengyang Normal University

Published on: 26 Oct 2020 - bioRxiv (Cold Spring Harbor Laboratory)

Topics: Ovary (botany) and Anaxagorea

Serial Section-Based 3D Reconstruction of *Anaxagorea* Carpel Vasculature and Implications for Integrated Axial-Foliar Homology of Carpels

Ya Li,[1,†] Wei Du,[1,†] Ye Chen,[2] Shuai Wang,[3] Xiao-Fan Wang[1,*]

1 College of Life Sciences, Wuhan University, Wuhan 430072, China

2 Department of Environmental Art Design, Tianjin Arts and Crafts Vocational College, Tianjin 300250, China

3 College of Life Sciences and Environment, Hengyang Normal University, Hengyang 421001, China

*Author for correspondence. E-mail: wangxf@whu.edu.cn

† Both authors contributed equally to this work

Running Title: Integrated Axial-Foliar Homology of Carpel

Abstract

The carpel is the basic unit of the gynoecium in angiosperms and one of the most important morphological features differentiating angiosperms from gymnosperms; therefore, carpel origin is of great significance in the phylogeny of angiosperms. However, the origin of the carpel has not been solved. The more recent consensus favors the interpretation that the ancestral carpel is the result of fusion between an ovule-bearing axis and the phyllome that subtends it. Since it has been confirmed by morphological and molecular evidence that foliar homologous are involved in carpel evolution, if axial homologs can be traced in the carpel, it would more likely be derived from an integrated axial-foliar structure.

This study aimed to reveal the axial structures in carpels by analyzing the continuous changes in vasculature from the receptacle to the carpels and ovules. *Anaxagorea* is the most basal genus of the primitive angiosperm Annonaceae. The conspicuous carpel stipe at the base of each carpel makes it an ideal material for exploring the possible axial homologous structure in the carpel. In this study, floral organogenesis and the topological vasculature structure were delineated in *A. luzonensis* and *A. javanica*, and a 3D-model of the carpel vasculature was reconstructed based on the serial sections.

The results show that (1) At the flowering stage, the number of vascular bundles entering each *Anaxagorea* carpel from the receptacle was significantly more than three, arranged in a radiosymmetric pattern, forming a basal ring at the base of each carpel. (2) All the carpel bundles are only connected with the central stele. (3) At the slightly upper part of the carpel, all the lateral bundles from the basal ring were reorganized into two groups, each forming a lateral bundle complex below each placenta. Bundles in each lateral bundle complex are also ring-arranged. (4) The ovule bundles were composed of non-adjacent bundles in the lateral bundle complex.

The composite origin of carpels is helpful to understand the composite origin of ovules. This study suggested that the circular arrangement of bundles in the receptacle, the carpel stipe, and the placenta of *Anaxagorea* are the consistent preferences in support of the theory that the carpel originates from an integrated axial-foliar structure. Despite more evidence is still needed to confirm that the circular arrangement of vascular bundles occurs only in the axial homologous structure.

Key words: 3D reconstruction; *Anaxagorea*; angiosperms; organogenesis; origin of the carpel; vascular anatomy

INTRODUCTION

Since Darwin's time, the elucidation of angiosperm origin and its evolutionary success has been a primary goal of plant science (Kennedy and Norman, 2005). The term "angiosperm" is derived from the Greek words angeion, meaning "container," and sperma, meaning "seed." Therefore, the carpel, an angiosperm-specific "seed container", is the definitive characteristic of angiosperms. The carpel is the basic unit of the gynoecium; it protectively surrounds the ovules by enclosing and sealing off their rims or flanks (Dunal, 1817; Robinson-Beers, 1992; Endress, 2015). The evolution of the carpel sets angiosperms apart from other seed plants, which develop exposed ovules. Previous studies have attempted to identify the potential angiosperm ancestors through phylogenetic analyses based on fossil, morphological, and molecular data. In these studies, particular emphasis was placed on assessing which ovule-bearing structures of various seed plants could be transformed into carpels. However, due to early differentiation, the extant angiosperms and gymnosperms underwent a long independent evolutionary process that resulted in the reproductive structure of the basal angiosperms and extant gymnosperms being significantly different, although some species of the two groups may have undergone convergent evolution (Winter et al., 1999; Soltis et al., 2002; Magallon et al., 2015). As a result, the origin of the carpel has not been solved.

The ancestral carpel is either interpreted as a conduplicate leaf-like structure bearing marginal ovules, or as the result from the integration of the ovule-bearing axis and the foliar appendage. Based on developmental evidence and functional genetics studies, the more recent consensus seems favoring the latter interpretation. (Skinner et al., 2004; Doyle, 2008; Wang, 2010, 2018; Mathews and Kramer, 2012; Liu et al., 2014; Zhang et al., 2017; Zhang et al., 2019). Owing to the difference between the two interpretations, it is important to determine whether the ovule-bearing axis is involved in the evolution of carpel. Since it has been confirmed by morphological and molecular evidence that foliar homologs are involved in the evolution of the carpel, if axial homologs can be found in the carpel, it would more likely have been derived from an integrated axial-foliar structure.

In this study, two *Anaxagorea* (Annonaceae) species were selected for floral organogenesis and vascular anatomic examination. Annonaceae represents one of the largest families in the Magnoliales that is one of the most important lineages in the early radiation of angiosperms (Sauquet et al., 2003), while *Anaxagorea* is the most basal genus of Annonaceae (Doyle and le Thomas, 1996; Doyle et al., 2004; Chatrou et al., 2012; Chatrou et al., 2018). *Anaxagorea* carpels are apocarpous (free) throughout their life history (Deroin, 1988), and each has a notably long carpel stipe (Endress and Armstrong, 2011). The microscopic observation of *Anaxagorea* tissue sections could determine whether there are "axial homologs" in the carpel and provide additional carpel origin evidence.

MATERIALS AND METHODS

Scanning Electron Microscopy and Paraffin Sectioning

Anaxagorea luzonensis flower samples at different floral stages (from early bud to young fruit) were collected from the Diaoluo Mountain, Hainan, China, in July 2017 and *Anaxagorea javanica* from the Xishuangbanna Tropical Botanical Garden, Yunnan, China in May 2017. The gynoecia were isolated and preserved in 70% formalin-acetic acid-alcohol (5:5:90, v/v), and the fixed specimens were dehydrated in a 50% to 100% alcohol series. To delineate the structure and development of the carpel, carpels were removed from the gynoecia, passed through an iso-pentanol acetate series (SCR, Shanghai, China), critically point-dried, sputter-coated with gold, observed, and photographed under a scanning electron microscope (Tescan VEGA-3-LMU, Brno, Czech Republic). Flowers and carpels were embedded in paraffin, serially sectioned into 10–12-µm thick sections, and stained with Safranin O and Fast Green to illustrate the vasculature. The transverse sections were examined and photographed using a bright-field microscope (Olympus BX-43-U, Tokyo, Japan). In addition, longitudinal hand-cut sections were made and observed for a rough check and better understanding of the vasculature.

Topological Analysis of Carpel Vasculature

Consecutive paraffin sections, 12-µm each, of *A. javanica* were stained with aniline blue, examined and photographed after excitation at 365 nm using an epifluorescence microscope (Olympus BX-43-U, Tokyo, Japan) and a semiconductor refrigeration charged coupled device (RisingCam, MTR3CMOS). Forty-five images were selected equidistant from the 423 sections taken for the 3D reconstruction. The figures were organized according to the vascular bundle outlines of the sections by using Adobe Photoshop CC 2017 and Illustrator CC 2017. The xylem and phloem contours were manually drawn, extracted as paths with the pen tool, and exported in DWG format. The DWG files were imported into 3Ds Max 2016 and sorted according to the distance and order of the sections. The paths were converted to Editable Spline curves to generate the basic modeling contour. The Loft command of Compound Objects was used to get the shape of the Editable Spline, and a complete 3D carpel vasculature model was generated.

RESULTS

Gynoecium Structure and Carpel Organogenesis

The flowers of two study species were trimerous with a whorl of sepals, two morphologically distinct whorls of petals, and numerous stamens (and inner staminodes of *A. Javanica*) (**Figures 1A–D**).

A. luzonensis usually exhibits two to four completely separate carpels (**Figures 1A, G**). The carpel primordia are almost hemispherically initiated and larger than the stamen primordia (**Figure 1F**). Each carpel consists of a plicate zone, a very short ascidiate zone (**Figures 3G, 5I, J**), and a long, conspicuous stipe (**Figure 2F**). The carpel stipe ontogenesis at the early stages of the carpel (**Figure 2B**). The continuous growth of the flanks on the ventral side of the young carpel triggers its early closure; however, the closure does not extend to the base of the carpel, where the carpel stipe occupied (**Figure 2C**). Subsequently, the dorsal region of each carpel thickens markedly, and the stigma forms (**Figures 2D, E**). At anthesis, the carpels are widest at

the basal region with an arch on the abaxial side. The carpel stipe remains elongate, accounts for approximately a quarter of the carpel length at anthesis, and continues to elongate during the fruiting stage (**Figure 1F**). Each carpel has two lateral ovules with the placentae at the ovary base (**Figures 3H, 5L**).

A. Javanica exhibits a multicarpellate gynoecium (**Figures 1B, J**). The carpels are completely separate and appear whorled at initiation (**Figure 1I**); as the carpel volume increases, the whorled structure becomes less obvious because the space in floral apex becomes limited. Each carpel consists of a plicate zone and a conspicuous carpel stipe (**Figure 2J**) but lacks the short ascidiate zone. The carpel stipe ontogenesis in the early stages (**Figure 2H**) and remains elongate during the flowering and fruiting stages (**Figures 1D, 2I–J**). Each carpel has two lateral ovules.

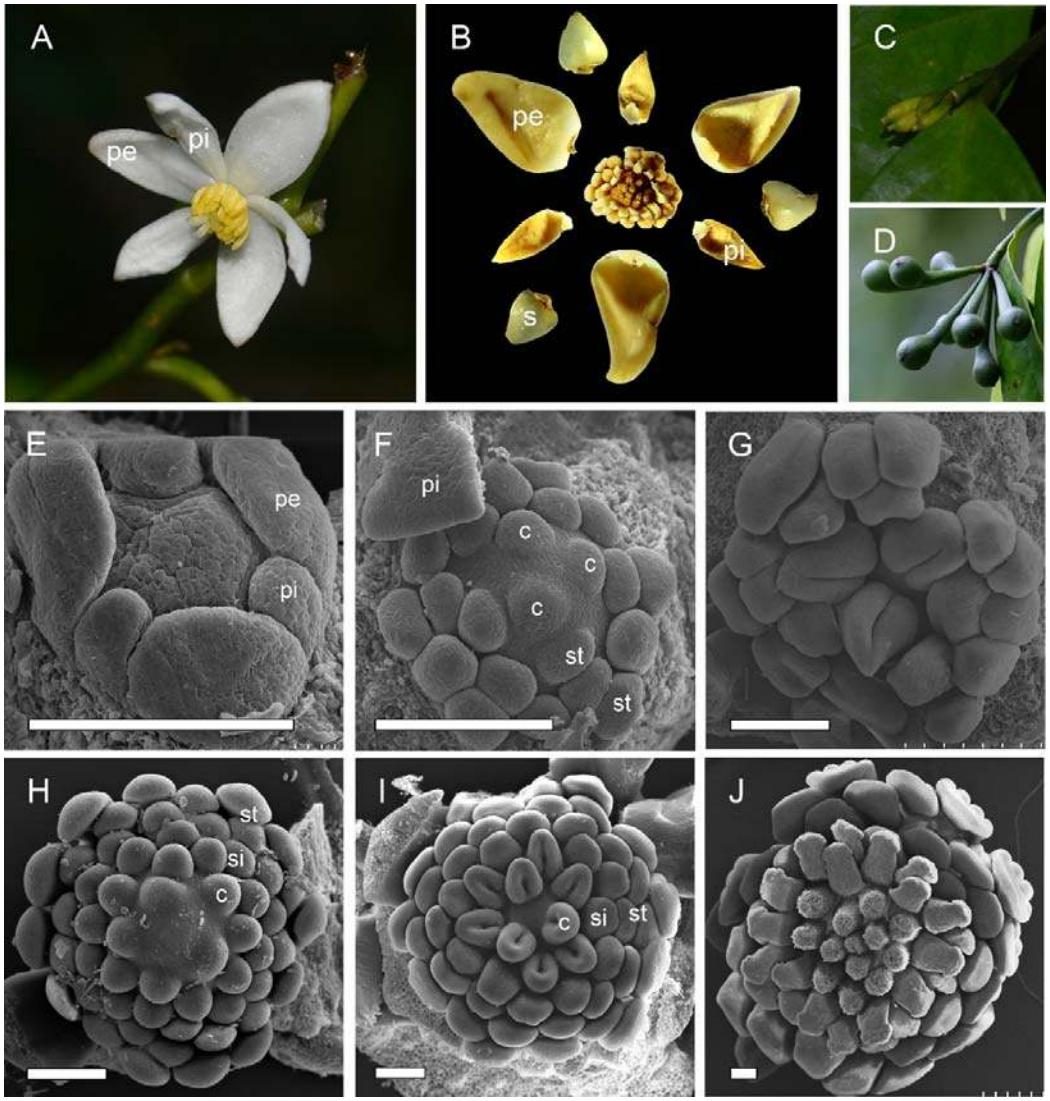

FIGURE 1. Floral morphology and gynoecium development in two *Anaxagorea* species. **(A)** *Anaxagorea luzonensis* flower. **(B)** *Anaxagorea javanica* flower. **(C)** Young *A. luzonensis* fruit. **(D)** Mature *A. javanica* fruit. **(E–G)** *A. luzonensis* floral development. **(H–J)** *A. javanica* gynoecium development. s, sepal; pe, outer petal; pi, inner petal; st, stamen; si, staminode; c, carpel. Scale bars =200 μm.

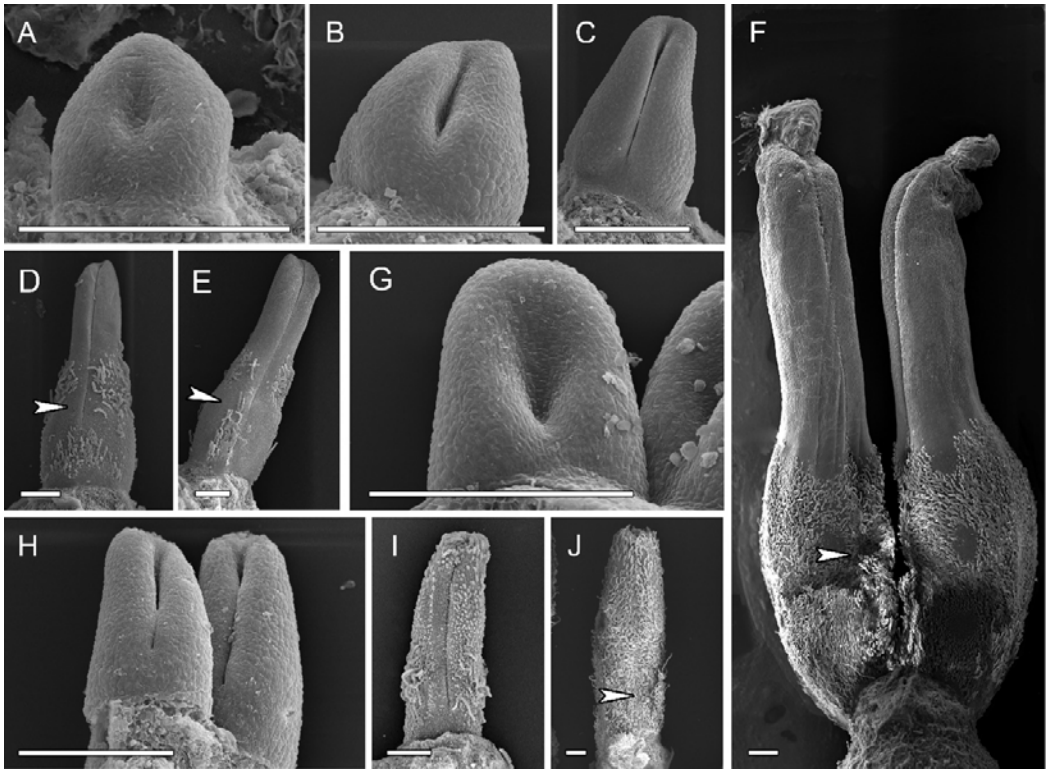

FIGURE 2. Carpel organogenesis in two *Anaxagorea* species. **(A–F)** *A. luzonensis.* **(A)** Carpel primordia. **(B–C)** Carpel stipe emergence. **(D–E)** Carpel thickening and stigma formation, showing carpel stipe elongation. **(F)** Mature carpels. **(G–J)** *A. javanica* shows similar carpel developmental features to changes depicted in **A–E, F**. Ventral slit end indicated by arrows. Scale bars = 200 μm.

174 **Vasculature from Receptacle to Carpel**

175 In the *A. luzonensis* cross-sections, the receptacle base presented a hexagon of 18
176 bundles from the pedicel stele (**Figure 3A**). The hexagon had six breaks, which built
177 up a crown of the cortical vascular system to supply the sepals and the two whorls of
178 petals and the stamens (**Figures 3B**). The central stele, composed of 18 bundles,
179 finally broke into two 9-bundle groups at the floral apex and ran into the 2-carpel
180 gynoecium (**Figures 3C, D**). Each group of nine bundles assembled as a basal ring
181 around the parenchyma at each carpel base (**Figures 3E**). At the slightly upper part of
182 each carpel, several bundles emerged on the lateral side, and the basal ring broke,
183 from which the dorsal bundle separated and the lateral bundles reorganized into two
184 groups of lateral bundle complexes (**Figures 3F**). In each of the lateral bundle
185 complexes, the adjacent bundles tended to join, assembling into an amphicribral
186 pattern (the xylem surrounded by the phloem) **Figure 3G**. Below each placenta, each
187 of the amphicribral lateral bundle complexes transformed into a set of "C"-shaped
188 lateral bundle complexes, from which the ovule bundles separated, while the other
189 bundles ran into the ovary wall. There were no horizontal connections between the
190 dorsal and other bundles (**Figure 3H**).
191
192 The pseudosteles at the base of the *A. Javanica* receptacle were triangular, with ~ 45
193 bundles. The outer six cortical traces were cylindrical and served the sepals and petals
194 (**Figures 4A, B**). At a slightly higher level, the androecial bundles emerged and
195 served the stamens by repeated branching, and the staminode bundles emerged as a
196 crown around the central stele (**Figure 4C**). Before entering the gynoecium, the
197 central stele enlarged and broke up into ~ 70 bundles to supply the nine carpels, and
198 each carpel was served by 7–10 bundles (**Figures 4D–E**). The vascular bundle
199 arrangement was similar to ascending sections in *A. luzonensis*, with the basal ring
200 and amphicribral lateral bundle complexes presented in each carpel (**Figures 4F–H**).
201

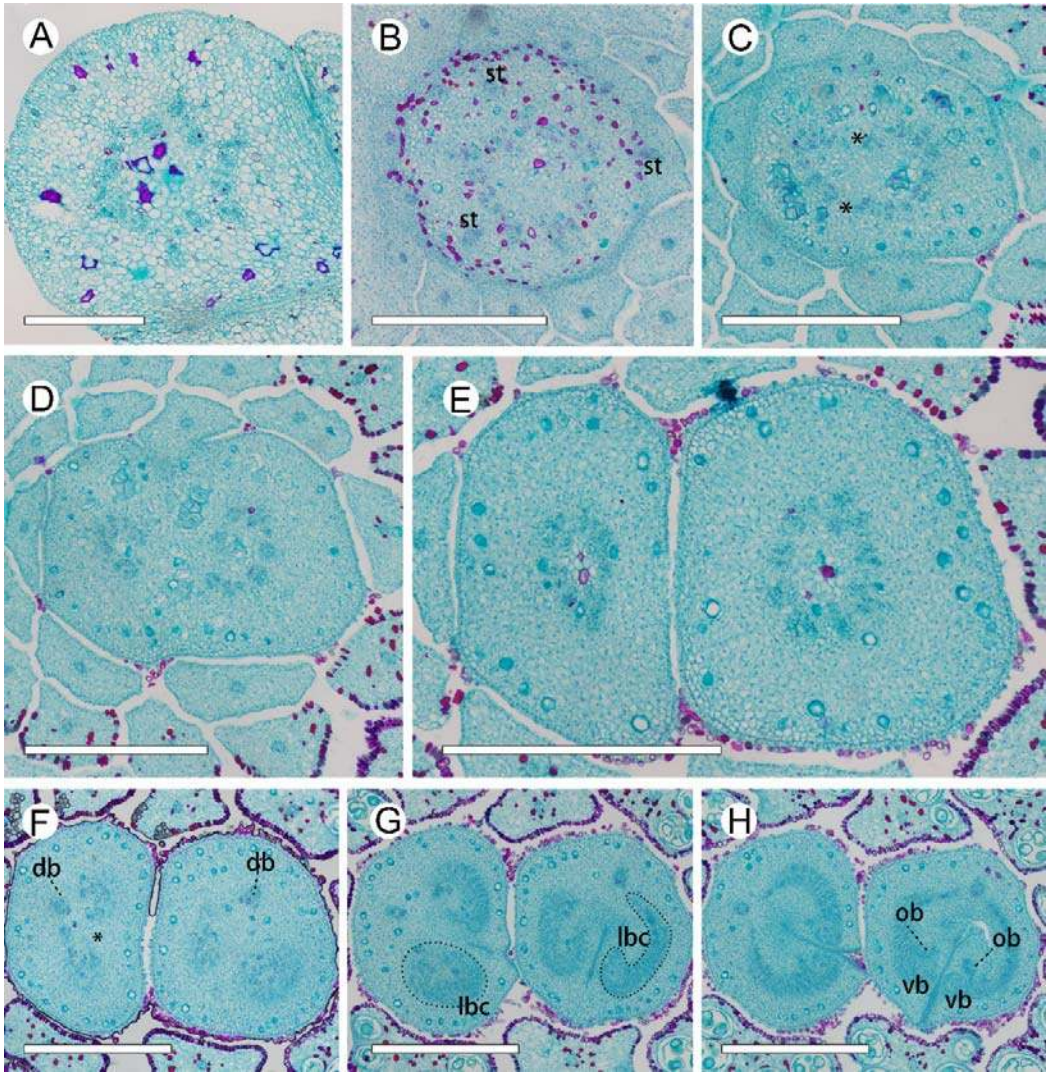

FIGURE 3. Ascending paraffin transections of *A. luzonensis* flower. **(A)** Base of receptacle. **(B)** Mid-section of androecia, showing stamen bundles and central stele. **(C)** Top of receptacle, showing central stele divided into two groups (* marked the breaks). **(D)** Bundles from the central stele enter carpels. **(E)** Base of carpels, showing basal ring. **(F)** Upper part of carpel stipes, showing the basal ring breaks (marked as *). **(G)** Bottom of ovary locule, showing amphicribral lateral bundle complexes (left) and "C"-shaped lateral bundle complexes (right). **(H)** Base of ovary locule. st, stamen; db, dorsal bundle; lbc, lateral bundle complex; vb, ventral bundle; ob, ovule bundle. Scale bars = 500 μm.

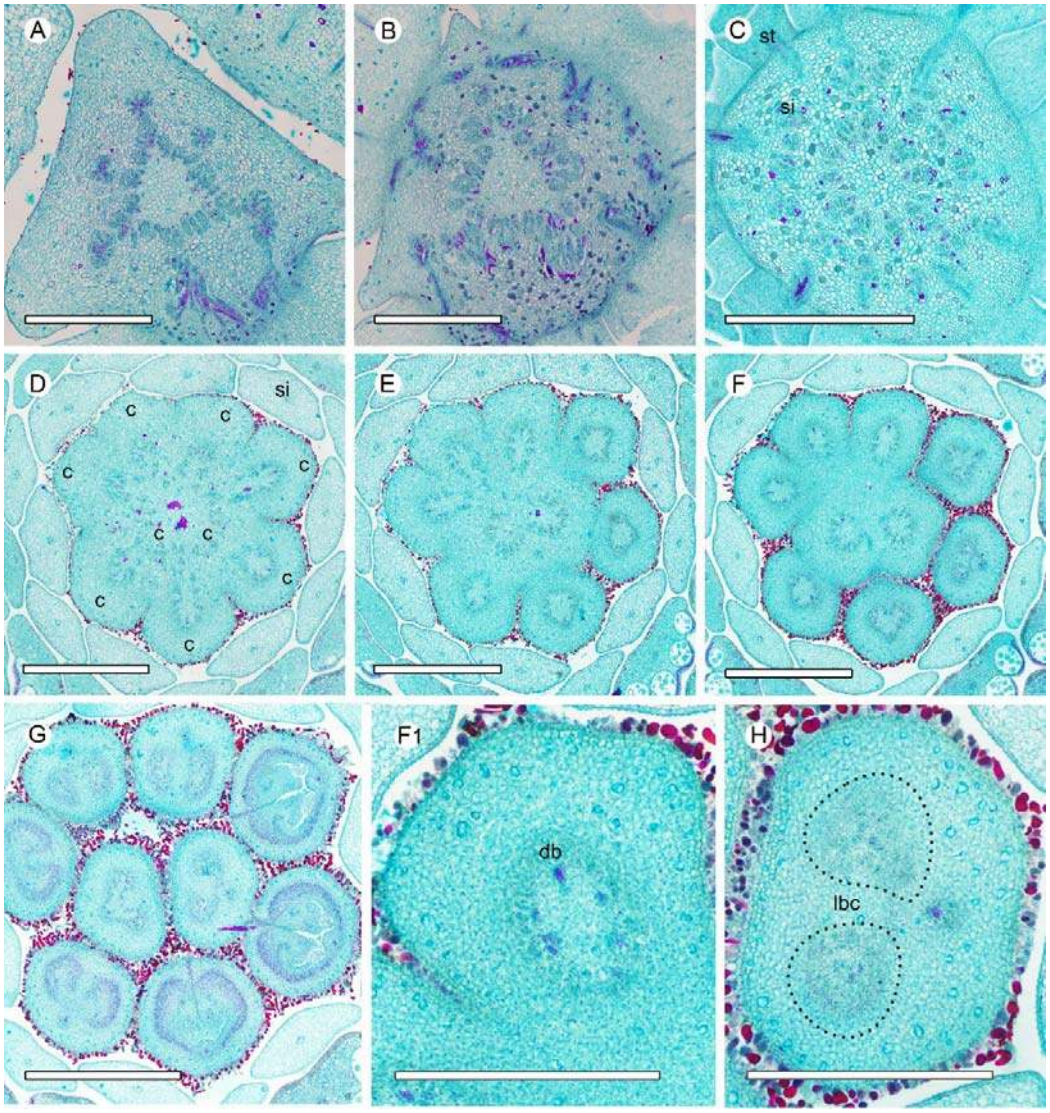

FIGURE 4. Ascending paraffin transections of *A. javanica* flower. **(A)** Base of receptacle, showing six groups of vascular bundles and sepal connections. **(B)** Points of petal connection to receptacle, showing perianth bundles. **(C)** Androecial bundles serving stamens by repeated branching. **(D–E)** Base of gynoecium, showing enlarged central stele breaks and bundles distributed into carpels. **(F–G)** Carpel vasculature at different positions. **(F1)** Detailed view of **(F)**, showing basal ring of carpel. **(H)** Amphicribral lateral bundle complexes in carpel. st, stamen; si, staminode; c, carpel; db, dorsal bundle; lbc, lateral bundle complex. Scale bars = 500 μm.

3D-Reconstruction of Carpel Vascular Topology

At the base of a mature *A. luzonensis* carpel, 15 discrete bundles were arranged in a radiosymmetric pattern, forming a basal ring around the central parenchyma (**Figure 5A**). At the slightly upper part, the basal ring curved inward on the ventral side and broke away from the invagination (**Figures 5B, C**). The bundles (except the dorsal) divided into two groups on each side of the carpel, each forming a lateral bundle complex, which was also ring-arranged. At the flowering stage, the lateral bundle complexes corresponded to the above-mentioned sections of the amphicribral complexes (**Figures 5D–F**). Below each placenta, bundles of each lateral bundle complex broke up on the dorsal side and transformed into a "C"-shaped lateral bundle complex (**Figures 5G, H**). The bundles on the ventral side of each lateral bundle complex gathered together (excluding the ventral bundle) and entered each ovule, while other bundles entered into the ovary wall. The ovule bundles are amphicribral. (**Figures 5I–L**).

Consecutive cross-sections of *A. Javanica* were similar in vasculature to those of *A. luzonensis* (**Figures 6A–D**). The base of the mature *A. Javanica* carpel exhibited 16 distinct bundles forming the basal ring (**Figure 6A, F**). The 3D model showed that (1) the basal ring and lateral bundle complex were cylindrical (**Figures 6F, H**). (2) The ovules were fed directly by bundles from the base of the carpel. (3) Each ovule bundle was formed from several non-adjacent lateral bundles distributed both relatively dorsally and laterally, and in which two bundles of them that fed each ovule were joined on the ventral side (**Figures 6G–I**). (4) The dorsal bundle remained independent throughout ontogenesis, without any link to other bundles (for details, please refer to the supplemental data).

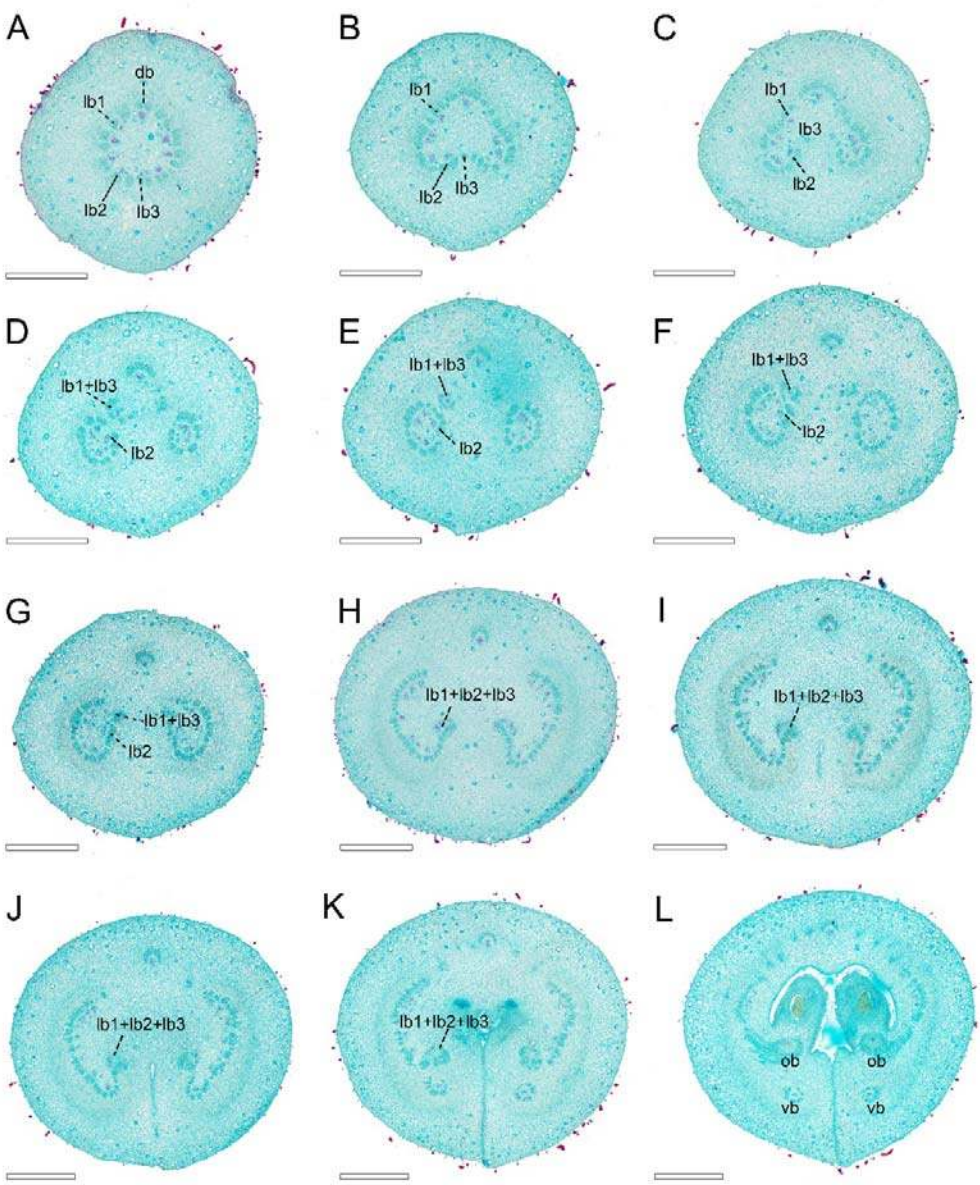

FIGURE 5. Ascending paraffin transections of mature *A. luzonensis* carpel. **(A)** Carpel base, showing basal ring. **(B–C)** Basal ring breaks on ventral side. **(D–F)** Ascending carpel stipe sections, showing lateral bundles reconstituted to two sets of ring-arranged lateral bundle complexes. **(G–H)** Top of carpel stipe, showing "C"-shaped lateral bundle complex. **(I–K)** Below ovary locule, showing formation of ovule bundles. **(L)** Base of ovary locule. db, dorsal bundle; lb, lateral bundle; vb, ventral bundle; ob, ovule bundle. Scale bars = 500 μm.

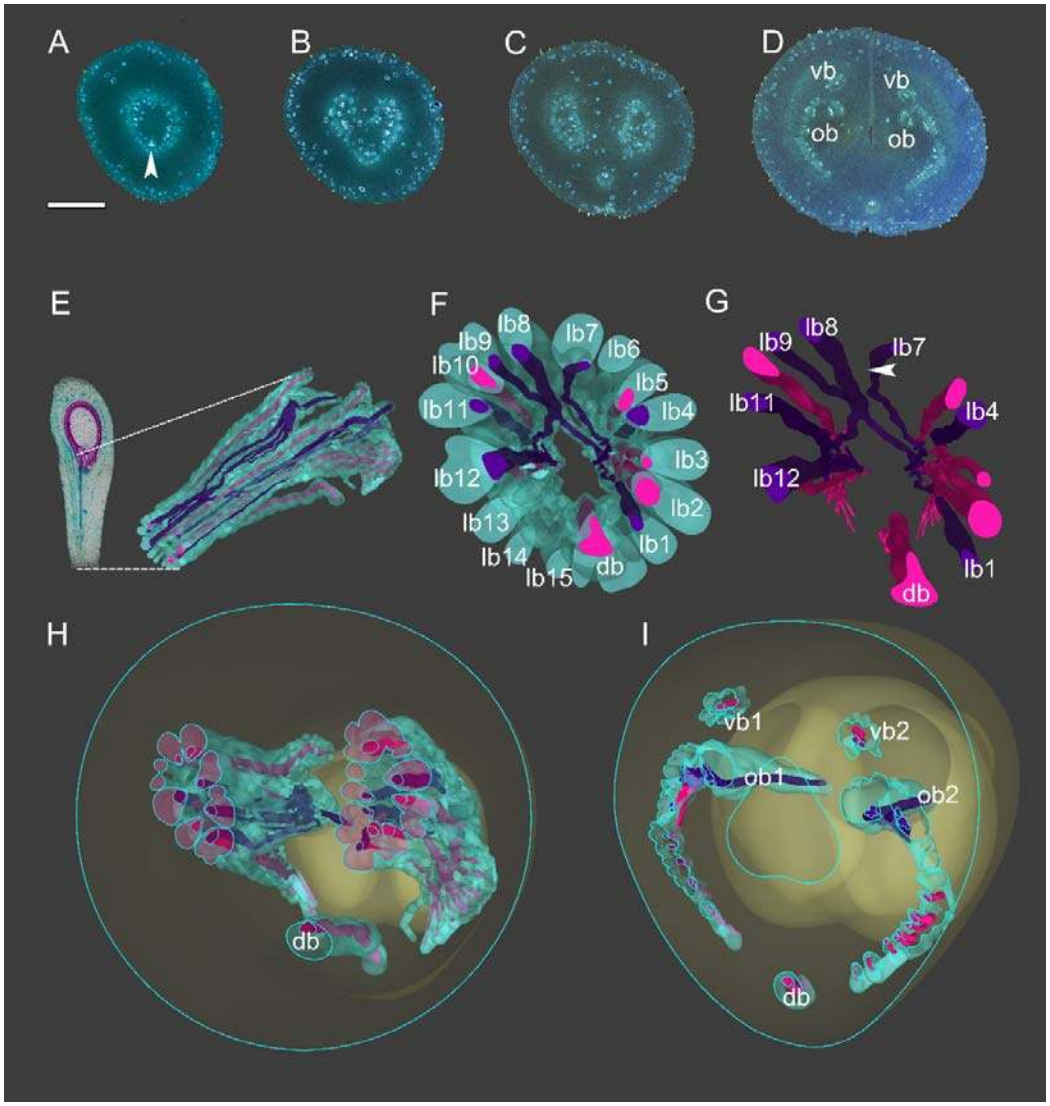

FIGURE 6. 3D construction of *A. javanica* vasculature.

Bundle outlines colored green, xylem red, and purple, among which bundles associated with ovule bundles are colored purple. **(A–D)** Aniline blue-stained *A. javanica* sections for modeling. **(E)** Longitudinal section of mature *A. javanica* carpel (left) and 3D vasculature model, dotted lines on longitudinal section indicate vasculature position in carpel. **(F)** Perspective from base of carpel vasculature. **(G)** Perspective from base of carpel (xylem only). The arrow indicates the intersection of two lateral bundles which fed two ovules. **(H)** Cross-section of 3D model corresponding to **(C)**, showing ring-arranged lateral bundle complexes. **(I)** 3D model section showing distribution of vascular bundles at base of ovary. db, dorsal bundle; vb, ventral bundle; ob, ovule bundle, lb, lateral bundle. Scale bars = 500 μm.

DISCUSSION

In this study, 3D reconstruction was used for the first time to reveal the *Anaxagorea* carpel vasculature, providing an analytical solution to the complex spatial relationship of floral organ vasculature. It is also the first time that the basal ring and the ring-arranged lateral bundle complex in the carpel have been reported. Observations on the continuous changes in vasculature from the receptacle to the carpel showed that the ring-arranged vasculature pattern was topologically continuous and repeatedly presented in the pedicel, the receptacle, the base of the carpel, and the placenta.

Anaxagorea Carpel Organogenesis

Peltate carpels have been suggested to be plesiomorphic in Annonaceae (Deroin, 1988; Igersheim and Endress, 1997; Surveswaran et al., 2010; Couvreur et al., 2011) and in some studies, *Anaxagorea* carpels have been reported to exhibit an ascidiate base (Deroin, 1988), while they have been described as completely plicate in others (Endress and Armstrong, 2011). In this study, floral organogenesis revealed that the carpel stipe emerges from the base of *A. luzonensis* and *A. javanica* carpels in the early stages of carpel development and elongate with the development of the carpel. In the flowering stage, the ventral slit of *A. luzonensis* terminates close to the base of the ovary locule, resulting in a very short ascidiate zone, while in *A. javanica*, it may continue below the ovary locule. These variations might suggest a transformation from peltate to plicate carpels in this genus. The specific carpel stipe of *Anaxagorea* provides a buffer for the drastic changes in carpel base vasculature and makes it an ideal material for exploring the possible axial homologous structure in the carpel.

Anaxagorea Floral Vasculature

Previous studies have reported that the Annonaceae gynoecium is fed by an enlarged central stele, and each carpel is usually fed by three bundles, one median and two lateral (Deroin, 1989; De Craene, 1993; Deroin and Norman, 2016; Deroin and Bidault, 2017). However, in *A. luzonensis* and *A. javanica*, the number of vascular bundles that fed the carpel during anthesis is significantly more than 3, regardless of the number of carpels, and the vascular bundles enter the *A. luzonensis* gynoecium is consistent with the central stele in numbers. The bundles entering the carpel are arranged in a radiosymmetric pattern, and this pattern maintains a spatiotemporal continuity throughout the carpel stipe. Considering that radiosymmetric vasculature is a universal feature in vascular plant stems (Metcalfe and Chalk, 1979; Evert, 2006; Beck, 2010; McKown and Dengler, 2010; Evert and Eichhorn, 2011), it is plausible that the basal ring represents the homology of the carpel and the axial structures. In the basal ring, there are two lateral bundles which fed to both ovules (lb8 and lb9 in **Figure 6G**), which makes the topological structure of the basal ring unable to be flattened as a leaf-like structure bearing marginal ovules.

It has been reported that in *Anaxagorea*, the ovules are served by the lateral bundle complex from the base of the carpel [e.g., *A. luzonensis* (Deroin, 1997); *A. crassipetala* (Endress, 2011)]. This pattern is different from most cases in Annonaceae, which has ovules served by separate vascular bundles branching directly from the

dorsal bundles [e.g., *Cananga* (Deroin and Le Thomas, 1989); *Deeringothamnus* (Deroin and Norman, 2016); and *Pseudartabotrys* (Deroin and Bidault, 2017)] or from relatively dorsally positioned bundles of the lateral network of bundles [e.g., *Meiocarpidium* (Deroin, 1987); and *Ambavia* (Deroin and Le Thomas, 1989)]. Our study showed that the topological structure of the ring-arranged lateral bundle complexes plays a key role in forming the ovule bundles and that it causes the non-adjacent bundles from the relatively dorsal and ventral sides to approach each other and merge. The dorsal bundle remained independent throughout, and there were no horizontal connections between it and the lateral bundle complexes. The ventral bundle took part in forming the spatial ring- arrangement of the lateral bundle complexes; however, it did not connect with the other bundles. These results indicate that the ovule and ovary wall bundles are relatively independent. This conclusion is also supported by previous studies that the ovule and ovary wall are controlled by two distinct, exclusive sets of genes (Angenent et al. 1995; Roe et al. 1997; Wynn et al. 2014).

Observation of the different development stages of the *Anaxagorea* carpel showed that the amphicribral bundle complexes in the placenta developed into the ring-arranged lateral bundle complexes with carpel maturation. In the vasculature development, the amphicribral bundles could be discrete inversely collateral bundles near the point of fusion, because their xylem portions need to approach each other before they become concentric (Endress, 2019). Based on derivation, the amphicribral bundles are frequently observed in small branches of early land plants, monocots, or immature young branches of dicots (Fahn, 1990). If the carpels are indeed derived from the integrated axial-foliar complex, that could explain why the amphicribral bundles are widely present in angiosperm placentae and funiculi [e.g., *Papaver* (Kapoor, 1973); *Psoraleae* (Lersten and Don, 1966); *Drimys* (Tucker, 1975); *Nicotiana* (Dave et al., 1981); *Whytockia* (Wang and Pan, 1998); *Pachysandra* (Von Balthazar and Endress, 2002); *Magnolia* (Liu et al., 2014); *Michelia* (Zhang et al., 2017); *Actinidia* (Guo et al., 2013); and *Dianthus* (Guo et al., 2017)].

In *Anaxagorea*, the central stele, the basal ring, the ring-arranged lateral bundle complex, and the amphicribral ovule bundle show similar topological properties to supports the view that the carpel originates from the integrated axial-foliar complex. The composite origin of carpels is helpful to understand the composite origin of ovules: how the bract-bracteole-terminal ovule system in the precursors of angiosperm evolved into an angiosperm carpel. However, the investigations in the present study were limited to a single genus. It is difficult to find similar morphological features in most angiosperms. Under natural conditions, terminal or axillary meristems can produce leaves and branches; however, the leaf meristem can only produce leaflets. The stimulus for vascular bundle formation comes from the base of the leaf primordium. If the carpel evolved from secondary reproductive shoots with foliar appendages, how does the female reproductive identity program interact with the meristems, what genetic pathways might interact with the development of the placenta and ovule formation, and are they shared in seed plants? To determine the structure from which carpels originated, we need more knowledge about functional

interaction between the primary meristem and the auxin flow coming from the leaf primodium to make sure whether the circular arrangement of vascular bundles occurs only in the axial homologous structure, and to further understand the molecular mechanisms of the various characteristics of carpel evolution.

AUTHOR CONTRIBUTIONS

YL planned and designed the research, performed the experiments, collected the images, drew the illustrations, and wrote the article; WD performed the experiments and complemented the writing; YC developed the 3D model; SW complemented the writing; X-FW supervised the experiments and complemented the writing.

FUNDING

This study was supported by the National Natural Science Foundation of China (grant number 31270282, 31970250).

ACKNOWLEDGMENTS

We thank Profs. Lars Chatrou, Xin Wang, and Xin Zhang for their helpful suggestions to the manuscript. We also thank Chun-Hui Wang, Shi-Rui Gan, and Yan-Lian Qiu for their help in searching for the target species in the field, Qing-Long Wang for his assistance in caring for the transplant materials in Hainan province, Qiang Liu for his support during sampling, and Lan-Jie Huang and Ke Li for their advice on manuscript writing. We would also like to thank Editage for English language editing.

REFERENCES

Angenent, G. C., Franken, J., Busscher, M., van Dijken, A., van Went, J. L., Dons, H. J., and van Tunen, A. J. (1995). A novel class of MADS box genes is involved in ovule development in *Petunia*. *Plant Cell* 7, 1569–1582. doi: 10.2307/3870020

Beck, C. B. (2010). *An Introduction to Plant Structure and Development: Plant Anatomy for the Twenty-first Century*, 2nd edn. Cambridge, New York: Cambridge University Press.

Chatrou, L. W., Pirie, M. D., Erkens, R. H. J. , Couvreur, T. L. P., Neubig, K.M., Abbott, J. R., et al. (2012). A new subfamilial and tribal classification of the pantropical flowering plant family Annonaceae informed by molecular phylogenetics. *Botanical Journal of the Linnean Society* 169, 5–40. doi:10.1111/j.1095-8339.2012.01235.x

Chatrou, L. W., Turner, I. M., Klitgaard, B. B, Maas, P. J. M., and Utteridge, T. M. A. (2018). A linear sequence to facilitate curation of herbarium specimens of Annonaceae. *Kew Bulletin* 73:39. doi: 10.1007/S12225-018-9764-3

Dave, Y. S., Patel, N. D., and Rao, K. S. (1981). Structural design of the developing fruit of *Nicotiana tabacum*. *Phyton* 21, 63–71.

De Craene, L. P. R., and Smets, E. F. (1993). The distribution and systematic relevance of the androecial character polymery. *Botanical journal of the Linnean Society* 113, 285–350. doi: 10.1111/j.1095-8339.1993.tb00341.x

Deroin, T. (1988). *Aspects anatomiques et biologiques de la fleur des Annonacées*. PhD Thesis. Centre d'Orsay: Université de Paris-Sud, France.

Deroin, T. (1989). Définition et signification phylogénique des systèmes corticaux floraux: l'exemple des Annonacées. *Comptes Rendus de l'Académie des Sciences, Paris* 308, Série III, 71–75.

Deroin, T., and Le Thomas, A. (1989). "Sur la systématique et les potentialités évolutives des Annonacées: cas d'*Ambavia gerrardii*," In: *espèce endémique de Madagascar*, Série III. ed. A. le Thomas. (*Comptes Rendus de l'Académie des Sciences Paris*) 309: 647–652.

Deroin, T. (1997). Confirmation and origin of the paracarpy in Annonaceae, with comments on some methodological aspects. *Candollea* 52: 45–58.

Deroin, T, and Norman, É. M. (2016). Notes on the floral anatomy of *Deeringothamnus* Small (Annonaceae): cortical vascular systems in a chaotic pattern. *Modern Phytomorphology* 9, 3–12.

Deroin, T., and Bidault, E. (2017). Floral anatomy of *Pseudartabotrys* Pellegrin (Annonaceae), a monospecific genus endemic to Gabon. *Adansonia* 39, 111–123. doi: 10.5252/a2017n2a2

Doyle, J. A., and Le Thomas, A. (1996). Phylogenetic analysis and character evolution in Annonaceae. *Adansonia* 18, 279–334.

Doyle, J. A., Sauquet, H., Scharaschkin, T., and Le Thomas, A. (2004). Phylogeny, molecular and fossil dating, and biogeographic history of Annonaceae and Myristicaceae (Magnoliales). *International Journal of Plant Sciences* 165, S55–S67. doi: 10.1086/421068

Doyle, J. A. (2008). Integrating molecular phylogenetic and paleobotanical evidence on origin of the flower. *International Journal of Plant Sciences* 169, 816–843. doi: 10.1086/589887

Dunal, M. F. (1817). Monographie de la famille des Anonacées. Paris: Treuttel & Würtz.

Endress, P. K., Armstrong, J. E. (2011). Floral development and floral phyllotaxis in

Anaxagorea (Annonaceae). *Annals of Botany* 108, 835–845. doi: 10.1093/aob/mcr201

Endress, P. K. (2005). Carpels in *Brasenia* (Cabombaceae) are Completely Ascidiate Despite a Long Stigmatic Crest. *Annals of Botany* 96, 209–215. doi: 10.1093/aob/mci174

Endress, P. K. (2015). Patterns of angiospermy development before carpel sealing across living angiosperms: diversity, and morphological and systematic aspects. *Botanical Journal of the Linnean Society* 178, 556–591. doi: 10.1111/boj.12294

Endress, P. K. (2019). The morphological relationship between carpels and ovules in angiosperms: pitfalls of morphological interpretation. *Botanical Journal of the Linnean Society* 189, 201–227. doi: 10.1093/botlinnean/boy083

Evert, R. F., and Eichhorn, S. E. (2013). *Raven Biology of Plants,* 8th edn. Palgrave Macmillan: W.H. Freeman Press.

Evert, R. F. (2006). *Esau's Plant Anatomy. Meristems, Cells, and Tissues of the Plant Body: Their Structure, Function, and Development,* 3rd edn. Hoboken, NJ: John Wiley & Sons, Inc.

Guo, X. M., Xiao, X., Wang, G. X., and Gao, R. F. (2013). Vascular anatomy of kiwi fruit and its implications for the origin of carpels. *Frontiers in Plant Science* 4, 391. doi: 10.3389/fpls.2013.00391

Guo, X. M., Yu, Y. Y., Bai, L., and Gao, R. F. (2017). *Dianthus chinensis* L.: the structural difference between vascular bundles in the placenta and ovary wall suggests their different origin. *Frontiers in Plant Science* 8, 1986. doi: 10.3389/fpls.2017.01986

Kapoor, L. D. (1973). Constitution of amphicribral vascular bundles in capsule of *Papaver somniferum*. Linn. *Botanical Gazette* 134, 161–165. doi: 10.1086/336698

Kaul, R. B. (1967). Development and vasculature of the flowers of *Lophotocarpus calycinus* and *Sagittaria latifolia* (Alismaceae). *American Journal of Botany* 54, 914–920. doi: 10.1002/j.1537-2197.1967.tb10715.x

Kennedy, D., and Norman, C. (2005) What don't we know? *Science* 309, 78–102. doi: 10.1126/science.309.5731.75

Lersten, N. R., and Don, K. W. (1966). The discontinuity plate, a definitive floral characteristic of the *Psoraleae* (Leguminosae). *American Journal of Botany* 53, 548–555. doi: 10.2307/2440004

Liu, W. Z., Hilu, K., and Wang, Y. L. (2014). From leaf and branch into a flower: *Magnolia* tells the story. *Botanical Studies* 55, 28. doi: 10.1186/1999-3110-55-28 doi: 10.1186/1999-3110-55-28

Magallon, S., Gomez-Acevedo, S., Sanchez-Reyes, L. L., et al. (2015). A metacalibrated time-tree documents the early rise of flowering plant phylogenetic diversity. *New phytologist* 207: 437–453 doi: 10.1111/nph.13264

Mathews, S. and Kramer, E. M. (2012). The Evolution of Reproductive Structures in Seed Plants: A Re-Examination Based on Insights from Developmental Genetics. *New phytologist* 194, 910–923. doi: 10.1111/j.1469-8137.2012.04091.x

McKown, A. D., and Dengler, N. G. (2010). Vein patterning and evolution in C4 plants. *Botany* 88, 775–786. doi: 10.1139/B10-055

Metcalfe, C. R., and Chalk, L. (1979). *Anatomy of the Dicotyledons, vol. 1, Systematic Anatomy of Leaf and Stem, with a Brief History of the Subject,* 2nd edn. Oxford: Clarendon Press.

Robertson, R. E., and Tucker, S. C. (1979). Floral ontogeny of *Illicium floridanum*,

with emphasis on stamen and carpel development. *American Journal of Botany* 66, 605–617. doi: 10.1002/j.1537-2197.1979.tb06264.x

Robinson-Beers, K., Pruitt, R. E., and Gasser, C. S. (1992). Ovule development in wild-type Arabidopsis and two female-sterile mutants. *Plant Cell* 4, 1237–1249. doi: 10.1105/tpc.4.10.1237

Sauquet, H., Doyle, J. A., Scharaschkin, T., Borsch, T., Hilu, K. W., Chatrou, L. W., et al. (2003). Phylogenetic analysis of Magnoliales and Myristicaceae based on multiple data sets: implications for character evolution. *Botanical Journal of the Linnean Society* 142, 125–186. doi: 10.1046/j.1095-8339.2003.00171.x

Skinner, D. J., Hill, T. A., Gasser, C. S. (2004). Regulation of Ovule Development. *Plant Cell* 16, S32–S45. doi: 10.1105/tpc.015933

Soltis, P. S., Soltis, D. E., Savolainen, V., Crane, P. R., and Barraclough, T. G. (2002). Rate heterogeneity among lineages of tracheophytes: Integration of molecular and fossil data and evidence for molecular living fossils. *Proceedings of the National Academy of Sciences* 99: 4430–4435. doi:10.1073/pnas.032087199

Tucker, S. C. (1975). Carpellary vasculature and the ovular vascular supply in *Drimys*. *American Journal of Botany* 62, 191–197. doi: 10.1002/j.1537-2197.1975.tb14052.x

Tucker, S. C. (1961). Phyllotaxis and vascular organization of the carpels in *Michelia fuscata*. *American Journal of Botany* 48, 60–71. doi: 10.1002/j.1537-2197.1961.tb11605.x

Von Balthazar, M., and Endress, P. K. (2002). Reproductive structures and systematics of Buxaceae. *Botanical Journal of the Linnean Society* 140, 193–228. doi: 10.1046/j.1095-8339.2002.00107.x

Wang, X. (2010). *The dawn angiosperms*. Heidelberg: Springer.

Wang, X. (2018). *The dawn angiosperms,* 2nd edn. Heidelberg: Springer.

Wang, Y. Z., and Pan, K. Y. (1998). "Comparative floral anatomy of *Whytockia* (Gesneriaceae) endemic to China," in *Floristic Characteristics and Diversity of East Asian Plants,* ed. A. L. Zhang, and S. G. Wu (Beijing: China Higher Education Press), 352–366.

Winter, K. U., Becker, A., Münster T., Kim, J. T., Saedler, H., and Theissen, G. (1999). MADS-box genes reveal that gnetophytes are more closely related to conifers than to flowering plants. *Proceedings of the National Academy of Sciences* 96: 7342–7347 doi: 10.1073/pnas.96.13.7342

Wynn, A. N., Seaman, A. A., Jones, A. L., and Franks R. G. (2014). Novel functional roles for PERIANTHIA and SEUSS during floral organ identity specification, floral meristem termination, and gynoecial development. *Frontiers in Plant Science* 5: 130. doi: 10.3389/fpls.2014.00130

Zhang, X., Liu, W., and Wang, X. (2017). How the ovules get enclosed in magnoliaceous carpels. *PLoS One* 12, e0174955. doi:10.1371/journal.pone.0174955

Zhang, X., zhang, Z. X. and Zhao, Z. (2019). Floral ontogeny of *Illicium Lanceolatum* (Schisandraceae) and its implications on carpel homology. *phytotaxa* 416, 200–210. doi: 10.11646/phytotaxa.416.3.1